Received: 5 October 2018 | Revised: 25 February 2019 | Accepted: 12 March 2019

DOI: 10.4218/etrij.2018-0550

ORIGINAL ARTICLE

WILEY ETRI Journal

Hierarchical sampling optimization of particle filter for global robot localization in pervasive network environment

Yu-Cheol Lee[1,2] | **Hyun Myung**[2,3]

[1]SW and Contents Research Laboratory, ETRI, Daejeon, Rep. of Korea

[2]Robotics Program, KAIST, Daejeon, Rep. of Korea

[3]School of Electrical Engineering, KAIST, Daejeon, Rep. of Korea

Correspondence
Hyun Myung, Robotics Program, KAIST, Daejeon, Rep. of Korea.
Email: hmyung@kaist.ac.kr

Funding information
This research was supported by the Ministry of Trade, Industry & Energy (MOTIE, Korea) under International Collaborative R&D Program N0002455, "ESTABLISH" in European Union Cluster ITEA3 Call2 (15008). This material is also partly based on work supported by the MOTIE under Industrial Technology Innovation Program No. 10067202, "Development of Disaster Response Robot System for Lifesaving and Supporting Fire Fighters in Complex Disaster Environment."

This paper presents a hierarchical framework for managing the sampling distribution of a particle filter (PF) that estimates the global positions of mobile robots in a large-scale area. The key concept is to gradually improve the accuracy of the global localization by fusing sensor information with different characteristics. The sensor observations are the received signal strength indications (RSSIs) of Wi-Fi devices as network facilities and the range of a laser scanner. First, the RSSI data used for determining certain global areas within which the robot is located are represented as RSSI bins. In addition, the results of the RSSI bins contain the uncertainty of localization, which is utilized for calculating the optimal sampling size of the PF to cover the regions of the RSSI bins. The range data are then used to estimate the precise position of the robot in the regions of the RSSI bins using the core process of the PF. The experimental results demonstrate superior performance compared with other approaches in terms of the success rate of the global localization and the amount of computation for managing the optimal sampling size.

KEYWORDS
global localization, mobile robot, particle filter, RSSI histogram bin, sampling optimization

1 | INTRODUCTION

The autonomous navigation services of mobile robots have been expanding in various fields such as logistics [1–3], guidance [4,5], and surveillance [6,7]. Recently, owing to the emergence of the pervasive network environment, new applications of mobility services have become feasible in multi-robot navigation [8,9], advanced human interaction [10], cloud intelligence [11], etc. The robots can exploit opportunities to improve core technologies by using pervasive network devices [12]. This study focuses on solving the problems of available autonomous navigation technologies (particularly the conventional localization algorithm) by providing a new hierarchical framework that can fuse measurements from robot-mounted sensors and pervasive network devices.

The navigation system of a mobile robot consists of various technologies such as localization, mapping, recognition, perception, path planning, and motion control [13,14]. As the core technology of navigation, the capability of determining the position of a robot is essential and has been studied in the field of localization methods.

This paper proposes a localization method of mobile robots that fuses different sensor information in order to achieve both a high success rate and an accuracy of global localization in a large space. We developed a hierarchical localization framework for mobile robots that can solve the problem of falling into the local minimum even with large computational

resources by managing the distribution effectively and determining the optimal size of samples. The main concept is to apply signals such as the received signal strength indication (RSSI) of Wi-Fi devices, to a stepwise localization framework in order to determine the global position of a robot. Recently, owing to the emergence of pervasive network technology, numerous mobile robots have employed a Wi-Fi-based network device as the fundamental equipment for communication covering workspaces; this enabled the implementation of various decentralized applications and services through a remote control system [15–17].

The localization framework consists of three major layers: the evaluation of RSSI bins, optimization of the population size of the samples, and estimation of position. Note that the RSSI bin is the fundamental unit of the prestored map including the radio signals and the obtained location. First, the RSSI bin evaluation can determine the coarse region where the robot is located, by matching the two data of the current signals of the RSSI measured by the Wi-Fi receiver and the bins of the map. Second, an optimization of the population size can regulate the total number of samples in the coarse region according to the evaluation results of the RSSI bins. Finally, the position estimation calculates the precise position of the robot in the coarse regions of the RSSI bins based on the optimized sample size by using the ranges of a laser scanner.

The proposed method contributes to achieving an accurate estimation of the robot position and to providing solutions for the issues with the conventional PF, such as being stuck in the local minimum and sampling size optimization. For preventing the local minimum, it limits the sample distribution to the region produced by the RSSI bins and reduces the likelihood of being stuck in false regions where the robot is not located. In addition, this can support rapid initialization for determining the robot's position in large-scale spaces. Meanwhile, the adjustment of the population size improves the performance of the diversity and the amount of computation. An adequate population size of the samples is used for successful initialization according to the evaluation results of the RSSI bins. The number of samples is then gradually reduced depending on the diversity of the sample distribution to save computational resources. This feature supports the localization capability of robots even with low-performance embedded boards in real time.

The remainder of this paper is organized as follows: After a discussion of the related work in the following section, Section 3 presents the hierarchical localization framework for estimating the position of a robot and adjusting the population size of the samples by using RSSI bins. Section 4 describes experiments and results to verify the effectiveness of the proposed method in terms of accuracy, success rate, diversity, and the amount of computation. Finally, the conclusions and future works are summarized in Section 5.

2 | RELATED WORK

Localization technology has advanced with various intelligent algorithms; these can be classified as either discrete or continuous approaches [18,19]. These two categories are different mainly in terms of the state representation. The continuous methods estimate the position of a robot with a single state and have been applied to mobile robot localization with substantial success in terms of accuracy and efficiency. The representative algorithms of the continuous approach include the Kalman filter [20,21], extended Kalman filter [22,23], and unscented Kalman filter [24]. Because these methods maintain only a single state, they are mainly used to track the position of the robot after the global localization [25].

The discrete methods secure the capability of estimating the global positions, even in a larger space, by using multiple states [26,27]. Popular algorithms using the discrete approach are Markov localization [28] and particle filter (PF) [29–34]. A PF operates multiple hypotheses based on a sample approximation method; this can overcome the limitation of the continuous approaches by using robust probabilistic models to reduce the effects of outliers. Generally, a PF is composed of four major steps for handling samples [18]: initialization, sampling, importance weight evaluation, and resampling. For stable localization in a large area, particularly to determine the initial global position, samples should be secured to cover the whole area. Otherwise, the PF frequently fails to determine the initial location because of falling into a local minimum. However, if numerous samples are used for the localization, the computational complexity may increase.

The trade-off between the sample size and amount of computation has hindered the implementation of global localization in a large-scale environment by using a PF [35]. In order to solve the problem wherein the sampling size becomes large depending on the space size, a PF has been developed to optimize the distribution and size of samples. The most representative approaches are the localization methods based on particle swarm optimization (PSO) and the Kullback-Leibler divergence (KLD) [36–38].

The PSO method can manage a sample distribution clustered in a group represented by individuals and thereby improve the efficiency of the sample size [39,40]. They consider the personal and global best values; these represent the fitness and the velocity of each individual, respectively. The PSO exhibits strong global search capability by using inertia weight, and its result is represented as the global best value. A PF based on PSO adjusts the sampling size in accordance with the global best value after determining the initial position in order to perform fast-tracking [41]. However, it is challenging to directly apply the PSO-based PF to determine

the initial position of the PF; this is because it cannot employ genetic operators such as mutation and crossover [42]. The mutation and crossover in the resampling process are the key aspects for managing the robustness of the distribution of the samples, particularly in the PF initialization. Although the number of particles can be reduced in the tracking process, it is challenging to use the PSO as a practical method of global localization; this is because it frequently fails to determine the initial position.

As an approach to optimizing the sample size and being able to apply mutation and crossover to the resampling process, the KLD method evaluates the quality of the sample distribution. This result is used for adjusting the sampling size. KL divergence, a stochastic model, provides a measure of the divergence of a probability from a second expected probability distribution [43]. The fundamental concept is based on two-layered evaluations. The first estimates the robot positions using the fitness value of the samples. This follows the fundamental processes of the PF. The second evaluates the divergences of the particle distribution to calculate the optimal sampling size. The latter step causes the problem of frequent falling into the local minimum when the robot has to determine the global position in a large-scale environment [44]. In the process of optimizing the sampling size, the excessive adjustment exerts a negative effect on the first step of position estimation, particularly on the accuracy and success rate of localization.

The hierarchical localization framework described in this paper resolves the problem of KLD wherein it fails to determine the global initial position owing to the excessive reduction in sampling size and the particle impoverishment. The proposed method determines the population size and the distributed region of the samples (rather than a statistical model such as the sample distribution of KLD) using the RSSI matching results of Wi-Fi signals. Because the RSSI value of Wi-Fi signals can better reflect the characteristics of the actual environment than the statistical model of KLD, the proposed method can optimize the sampling size more effectively; moreover, it can ensure a higher success rate of PF initialization compared with that of KLD.

3 | HIERARCHICAL LOCALIZATION FRAMEWORK

The localization framework described in this paper consists of three steps: RSSI bin evaluation, population size optimization, and position estimation, as illustrated in Figure 1. First, the process of RSSI bin evaluation selects the candidate region in which the robot is placed, by matching the current radio signals with the stored RSSI bins. Second, the population size optimization regulates the sampling size of the PF; this reduces the amount of computation necessitated by advanced diversity of the sample distribution in the PF. Finally, the position estimation step is a fundamental algorithm of the PF to accurately determine the position of the robot using the measurements by the odometer and laser scanner.

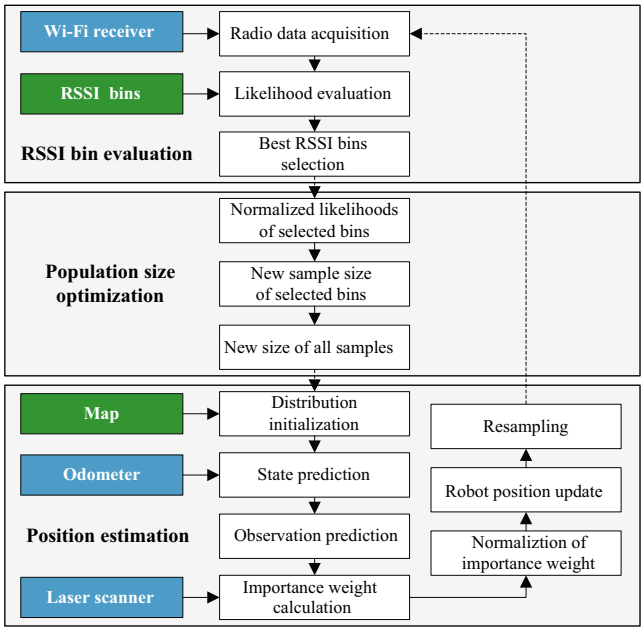

FIGURE 1 Schematic diagram of the hierarchical localization framework that consists of RSSI bin evaluation, population size optimization, and position estimation

This approach can improve the success rate of the initialization process of the PF with a reduced amount of computation. A larger sampling size can lower the possibility of the occurrence of the local minimum problem of the initialization; however, it requires larger computational resources to evaluate all the samples. The RSSI bin-based PF localization provides a solution to adaptively regulate the sampling size and robustly manage the diversity of the sample distribution so that the robot can accurately estimate the position in large-scale spaces with a small number of samples. The key concept is that the RSSI matching result provides the absolute regions that exhibit high possibilities for the presence of the robot; then, the PF can scatter the adaptive sizes of the samples covering only the regions of the selected RSSI bins. For stepwise localization, it ensures precise localization of the robot without the problems of a large amount of computation or of falling into a local minimum, encountered in the conventional PF.

3.1 | RSSI bin evaluation

The objective of the RSSI bin evaluation is to select the absolute and coarse areas with regard to the current position of the robot in the space.

3.1.1 | Radio data acquisition

The first step of the RSSI bin evaluation is accomplished by measuring the radio signals of Wi-Fi devices. Fundamentally, most robot platforms are equipped with a Wi-Fi receiver to share information, commands, status, etc., with other robots or servers. As an additional function in this study, the Wi-Fi receiver collects the observation of the radio signal ($\mathbf{r}^t$) at the current time t for localization as in

$$\mathbf{r}^t = \left\{ \left(m_j^t, r_j^t \right) | j = 1, \ldots, n_r^t \right\}, \tag{1}$$

where the data of the radio signal are composed of the n_r^t set with the MAC address m_j^t and the RSSI value r_j^t. The MAC addresses are used as identification to distinguish its RSSI values from other radio signals.

3.1.2 | Likelihood evaluation

This step calculates the total likelihood value by comparing the reference and the observation RSSI values corresponding to a MAC address. The group of RSSI bins ($\mathbf{B}^t$) defined as the n_b dataset with the RSSI bin ($\mathbf{b}_k^t$) is prebuilt reference information stored as the map in (2). Each RSSI bin consists of the center location of the region ($\hat{x}_k, \hat{y}_k$), radio signals ($\hat{\mathbf{r}}_k$), and likelihood value ($\hat{\lambda}_k^t$) as follows:

$$\mathbf{B}^t = \left\{ \mathbf{b}_k^t | k = 1, \ldots, n_b \right\}, \quad \mathbf{b}_k^t = \left(\hat{x}_k, \hat{y}_k, \hat{\mathbf{r}}_k, \hat{\lambda}_k^t \right). \tag{2}$$

A histogram matching method is used for evaluating the likelihood value of each RSSI bin. Histogram matching is a process wherein a time series or high-dimensional scalar data are modified such that its histogram matches that of a reference dataset [45]. In this paper, the current radio signal observation ($\mathbf{r}^t$) and the group of RSSI bins ($\mathbf{B}^t$) are defined as the high-dimensional scalar data and the reference dataset, respectively, for histogram matching.

The likelihood value of each RSSI bin is determined by using the residual between the reference and observation RSSI values, $\hat{r}_k$ and r_j^t, respectively, corresponding to the MAC address ($\hat{m}_k = m_j^t$) as follows:

$$\hat{\lambda}_k^t = p\left(\mathbf{r}^t; \mathbf{b}_k \right) = p\left(\mathbf{r}^t, \hat{\mathbf{r}}_k \right) = \prod_{j=1}^{n_r^t} p_r\left(r_j^t - \hat{r}_k \right),$$
$$p_r(\cdot) = \frac{1}{\sqrt{2\pi\sigma_r^2}} \exp \frac{\left(10^{\frac{-r_j^t}{20}} - 10^{\frac{-\hat{r}_k}{20}} \right)^2}{2\sigma_r^2}, \tag{3}$$

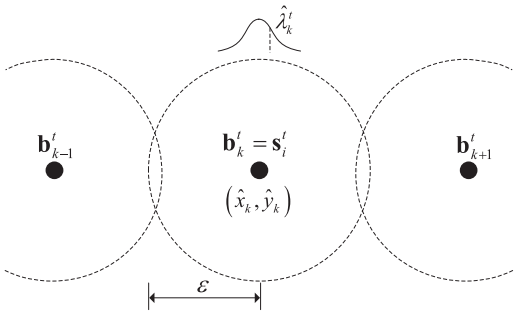

FIGURE 2 Concept of selecting RSSI bins to determine the coarse region where the robot is located; for example, if the likelihood value ($\hat{\lambda}_k^t$) is top ranked for the selected RSSI bins ($\mathbf{b}_k^t$), the coarse region is defined by the center location ($\hat{x}_k, \hat{y}_k$), and the error boundary of the bin (ε)

where $p_r(\cdot)$ is theoretically based on the Friis formula that supports the equation for transformation from the decibel unit of received radio power to the metric unit of distance [46]. By converting the RSSI from decibel unit to metric distance, the histogram matching is performed in a linear scale to respond to the metric location of the RSSI bin. In addition, $p_r(\cdot)$ is represented by the Gaussian distribution with the radio power variance σ_r^2.

3.1.3 | Best RSSI bins selection

This process determines the coarse-region candidates where the robot is located using the results of the likelihood evaluation. The group of the selected RSSI bins ($\mathbf{S}^t$) is defined as the top-s RSSI bins ($\mathbf{s}_i^t$) when the RSSI bins in the group ($\mathbf{B}^t$) are sorted in descending order according to the likelihood value ($\hat{\lambda}_k^t$) as:

$$\mathbf{S}^t = \{ \mathbf{s}_i^t | i = 1, \ldots, s \} = \left\{ \mathbf{b}_k^t \left| \underset{1 \le k \le s}{\arg\max} \left(\hat{\lambda}_k^t \right), \mathbf{b}_k^t \in \mathbf{B}^t, s = [\Sigma_f / \varepsilon] \right. \right\}, \tag{4}$$

where s is determined by the accuracy of the RSSI bin evaluation (Σ_f) and the error boundary of the bin (ε). In the physical domain, the region of Σ_f is covered by s RSSI bins.

As shown in Figure 2, if the likelihood value ($\hat{\lambda}_k^t$) is in the cutoff rank for selecting the best RSSI bins, its RSSI bin ($\mathbf{b}_k^t$) is designated as the element $\mathbf{s}_i^t$ and belongs to the group of selected RSSI bins ($\mathbf{S}^t$). The coarse region where the robot is located is defined by the center location ($\hat{x}_k, \hat{y}_k$) and the error boundary of the bin (ε) where ε is determined from several meters to dozens of meters. The main purpose of this step is

to determine the candidate areas where the robot is present; moreover, even if the error boundary is tens of meters in the worst case, it is not a critical problem for estimating the robot position.

For the next layers in the localization framework, the likelihood values of the selected RSSI bins are used for resizing the optimal number of samples to circumvent the need for a large amount of computation. The coarse region provides the boundary of scattering the samples to solve the problem of the local minimum in the large-scale space.

3.2 | Population size optimization

The population size of the samples is an important factor for the PF localization method with regard to the success of the initialization, computational resources, diversity management, etc. For successful initialization, the population size of the samples should be sufficient to cover the workspace. If the population size is not sufficient to cover the entire region with adequate diversity, the PF frequently falls into the local minimum and fails to initialize its localization process. On the contrary, an excessive population size causes an overflow effect, which results in computational complexity. This is a critical issue for real-time systems such as those for localizing mobile robots. Therefore, the population size of the samples is a key factor for the success of the PF and should be determined at an appropriate level according to various situations such as kidnapping, tracking, and obstacle avoidance.

To determine the optimal sample size, the group of all samples is defined as $\mathbf{Q}^t$, and the state of the i-th sample at time t ($\mathbf{q}_i^t$) is defined as a position (x_i^t, y_i^t, θ_i^t) and a weight (w_i^t) as

$$\mathbf{Q}^t = \left\{ \mathbf{q}_i^t \,\middle|\, i = 1, \ldots, n_q^t \right\}, \quad \mathbf{q}_i^t = \left(x_i^t, y_i^t, \theta_i^t, w_i^t\right). \tag{5}$$

The weight is the fitness value to evaluate the similarity between the sample position and real position. If the population size of the samples at t is n_q^t and the state of the sample is randomly placed on the map, the initial weight of each sample is set as $1/n_q^t$.

3.2.1 | Normalized likelihoods of selected bins

This process rescales the likelihood values so that the sum of the likelihoods for all the RSSI bins is 1. In the group of selected RSSI bins ($\mathbf{S}^t$), each likelihood is assigned as a normalized value (Δ_j) to reduce the effect on the different scales of the likelihood distribution as follows:

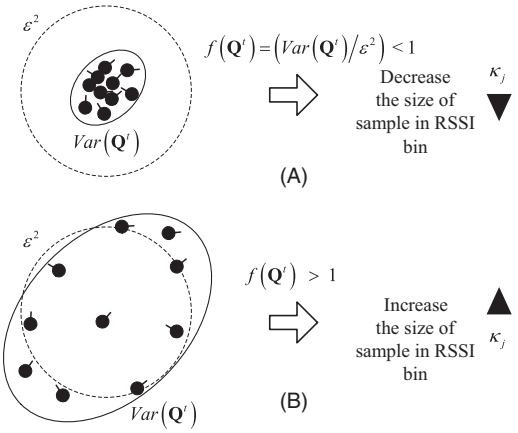

FIGURE 3 The concept of optimization of population size is based on the divergence evaluation, $f(\mathbf{Q}^t)$, to compare two distributions: the current variance of all the samples, $Var(\mathbf{Q}^t)$, and the error boundary of an RSSI bin, ε^2. (A) If the divergence $f(\mathbf{Q}^t)$ is smaller than 1, the population size is decreased at the subsequent iteration to eliminate the redundant samples over the small area. (B) If the divergence $f(\mathbf{Q}^t)$ is larger than 1, the population size is increased at the subsequent run to cover the wide region

$$\Delta_j = \hat{\lambda}_j^t \Big/ \sum_{k=1}^{n_b} \hat{\lambda}_k^t;\ \hat{\lambda}_j^t \in \mathbf{S}^t,\ \hat{\lambda}_k^t \in \mathbf{B}^t. \tag{6}$$

3.2.2 | New sample size of selected bin

This step is a key component for determining the appropriate population number of samples (κ_j) corresponding to the selected RSSI bin as follows:

$$\begin{aligned} \kappa_j &= \Delta_j \times \left(\frac{\varepsilon}{\delta}\right)^2 \times \left(\frac{2\pi}{\varphi}\right) \times f(\mathbf{Q}^t), \\ f(\mathbf{Q}^t) &= (Var(\mathbf{Q}^t)/\varepsilon^2), \end{aligned} \tag{7}$$

where the increase in the new sampling size is proportional to the normalized likelihood value (Δ_j). In addition, the parameters δ and φ are the physical resolutions of the distance and the angle bearing, respectively, between the different samples. The typical values of these two resolutions are obtained from the environmental complexity so that the samples cover the whole region. The function of divergence ($f(\mathbf{Q}^t)$) is an element that evaluates whether the distribution of the current samples ($Var(\mathbf{Q}^t)$) can cover the region corresponding to an RSSI bin (ε^2) as in Figure 3.

In contrast, the KLD method determines the number of samples based on the difference between a true distribution and a current particle density [36]. The true distribution is approximated by the statistical models because it cannot be

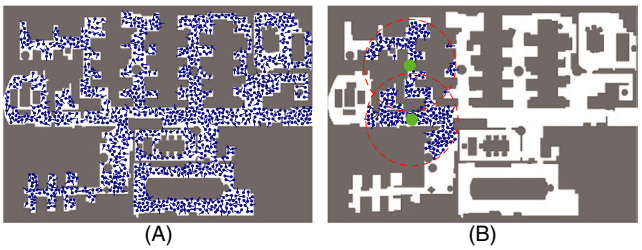

FIGURE 4 (A) The samples (blue color) are uniformly scattered on the map to start the PF. The total number of samples is 4,000. (B) The states of the samples are located in the error boundary of the selected RSSI bins (red dotted circles, $s = 2$). The initial position of the robot can be estimated with a small number of samples because the selected RSSI bins contain the coarse locations (green points) where the robot is located

inferred as an exact value when expressed as linear equations. In certain cases, the errors in the approximation result in a miscalculation of the true distribution and an acceleration of the particle depletion, further deteriorating the local minimum. To solve this issue, our proposed method uses the boundary of the RSSI bin of Wi-Fi signals (ie, a physical value rather than an approximation) as the true distribution. It can maintain the appropriate number of samples and robust distribution under all circumstances.

3.2.3 | New size of all samples

This step determines the total number of samples for accurately estimating the position within the selected RSSI bins. The new sample size (n_q^t) is calculated by the sum of the new sizes of all the selected RSSI bins as $n_q^t = \sum_{j=1}^{s} \kappa_j$.

3.3 | Position estimation

The PF localization can robustly provide accurate performance even under abnormal situations such as robot kidnapping, errors of sensor measurements, and obstacle collisions; this is because it has been developed to maintain an appropriate diversity of the sample distribution based on the stochastic theory.

The process of the PF localization to determine the robot locations consists of seven processes. First, the PF initializes the samples bounded in the selected RSSI bins to determine the starting location of the robot. Second, each state of the sample is predicted by the odometer data. Third, the distances of the laser scanner obtained from the predicted observations are calculated at the predicted state by using the map data. Fourth, the weight of each particle as the fitness level of the sample is evaluated by matching the predicted observation with the measurement by the laser scanner. Fifth, the weights of all the samples are normalized to resolve the scale effect correlated with the population size. Sixth, the current robot position is determined by the weighted sum of the states of the samples. Finally, the new samples are replicated according to the probability proportional to the weight; thus, the distribution of samples can robustly adapt to changes in the surrounding situations, such as kidnapping and dynamic obstacles.

3.3.1 | Distribution initialization

This process randomly seeds the samples to cover the regions of the selected RSSI bins by using the map data. As shown in Figure 4A, the samples can be placed only in the free region where the robot can move or stop. This condition contributes to reducing the population size of the samples to cover the area; however, it is not a fundamental solution to manage the sampling size in a large space. As the size of the space enlarges, the sampling size should be accordingly enlarged to prevent the local minimum problem. However, this simple strategy necessitates a large amount of computation.

Figure 4B shows the concept of the methodology to overcome the trade-off between the local minimum and the amount of computation using the selected RSSI bins. The states of the samples are assigned by using a random function $R(\cdot)$ only around the region of the selected RSSI bins (ε) as follows:

$$\mathbf{Q}^t = \sum_{j=1}^{s} \{R(\mathbf{q}_i) | 1 \le i \le \kappa_j\} : \begin{cases} |x_i^t - \hat{x}_j| \le \varepsilon, \\ |y_i^t - \hat{y}_j| \le \varepsilon, \\ |\theta_i^t| \le \pi, \end{cases} \tag{8}$$

where κ_j and $(\hat{x}_j, \hat{y}_j)$ are the allocated sampling size and the location of each selected RSSI bin, respectively. The constraint boundary of the selected RSSI bins scattering the samples contributes to solving the problem of the local minimum with a small population of samples, that is, small amount of computation, by reducing the search area; the larger the space is, the higher the probability that the area will have a similar structure. In addition, it can aid the rapid determination of the position of the robot in the initialization step.

3.3.2 | State prediction

This process predicts the current position $(x_i^t, y_i^t, \theta_i^t)$ of the sample at time t with the state model defined as

$$p(\mathbf{q}_i^t | \mathbf{q}_i^{t-1}, \mathbf{u}^t) = \begin{bmatrix} x_i^t \\ y_i^t \\ \theta_i^t \end{bmatrix} = \begin{bmatrix} x_i^{t-1} + d\cos(\theta_i^{t-1} + \Delta\theta_1) \\ y_i^{t-1} + d\sin(\theta_i^{t-1} + \Delta\theta_1) \\ \theta_i^{t-1} + \Delta\theta_1 + \Delta\theta_2 \end{bmatrix}. \tag{9}$$

In (9), the current position is calculated by the kinematic relationship between the previous position $(x_i^{t-1}, y_i^{t-1}, \theta_i^{t-1})$ and the control input $(\mathbf{u}_t)$. The control input consists of the distance (d) and the angles $(\Delta\theta_1, \Delta\theta_2)$ measured by the odometer when the robot moves from time $t-1$ to t. As shown in Figure 5, the state of the sample can be predicted based on the sequential motion variations; for the subsequent motion, vary the angle $(\Delta\theta_1)$ to the target location, move a certain distance (d), and vary the angle $(\Delta\theta_2)$. The predicted state of the sample is used in the subsequent step to extract the range measured by the laser scanner using the observation model.

3.3.3 | Observation prediction

This process anticipates the measurements $(\tilde{\mathbf{z}}_i^t)$ by the laser scanner at the predicted position of the sample. As shown in Figure 6, the observation model is based on the measurement principle of the laser scanner, which should detect the nearest object in the direction of the beam. The observation model can predict the n_z data pairs of the range $(\tilde{l}_j)$ and the bearing angle $(\tilde{\phi}_j)$ corresponding to the state of each sample as follows:

$$p(\tilde{\mathbf{z}}_i^t|\mathbf{q}_i^t, \mathbf{M}) = \begin{bmatrix} \tilde{l}_j \\ \tilde{\phi}_j \end{bmatrix} = \begin{bmatrix} \sqrt{(x_j - x_i^t)^2 + (y_j - y_i^t)^2} \\ \theta_i^t + \Delta\phi_j \end{bmatrix}, \quad (10)$$

where $j = 1, \ldots, n_z$, (x_j, y_j) is the location of the closest object in the laser beam line and $\mathbf{M}$ is the preconstructed grid map that represents the structure of space.

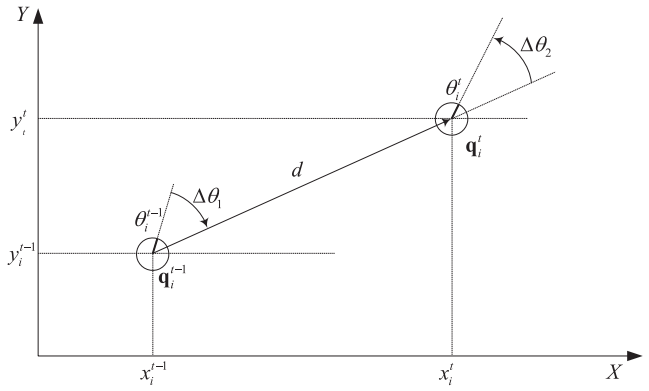

FIGURE 5 The state model predicts the position $(x_i^t, y_i^t, \theta_i^t)$ of the sample by using the previous position $(x_i^{t-1}, y_i^{t-1}, \theta_i^{t-1})$ and the control input $(\mathbf{u}^t)$. It is derived from a kinematic analysis of the robot movement. From the perspective of control, to move to the target position, the motion of the robot should consist of three steps: change direction $(\Delta\theta_1)$, move a certain distance (d), and rotate its orientation $(\Delta\theta_2)$ for the subsequent motion

3.3.4 | Importance Weight Calculation

This process evaluates the weight value (w_i^t) of each sample by calculating the likelihood between the predicted observation $(\tilde{\mathbf{z}}_i^t)$ and the actual measurement $(\mathbf{z}^t)$ as follows:

$$p(w_i^t|\tilde{\mathbf{z}}_i^t, \mathbf{z}^t) = \prod_{j=1}^{n_z} p(-|\tilde{l}_j - l_j^t|) \cdot p(-|\tilde{\phi}_j - \phi_j^t|), \quad (11)$$

where $p(\cdot) \approx N(0, \sigma^2)$. The likelihood function uses the residuals $(\tilde{l}_j - l_j^t, \tilde{\phi}_j - \phi_j^t)$ as the parameters for the Gaussian distribution $p(\cdot)$ with zero mean and variance σ^2. The larger the weight is, the more accurate the position of the sample.

3.3.5 | Normalization of importance weight

It is a convenient computation process to eliminate the impact of varying of the population size. The weight value of each sample (w_i^t) should be divided by the sum of the weight values of n_q^t samples as follows:

$$w_i^t \leftarrow w_i^t \Big/ \sum_{j=1}^{n_q^t} w_j^t. \quad (12)$$

Although the population size will be dynamically varied to maintain the diversity of the sample distribution, this process can normalize the influence of each sample to estimate the position of the robot.

3.3.6 | Robot position update

This process estimates the current position of the robot $(\mathbf{x}^t)$ by using the weight of the distributed samples as follows:

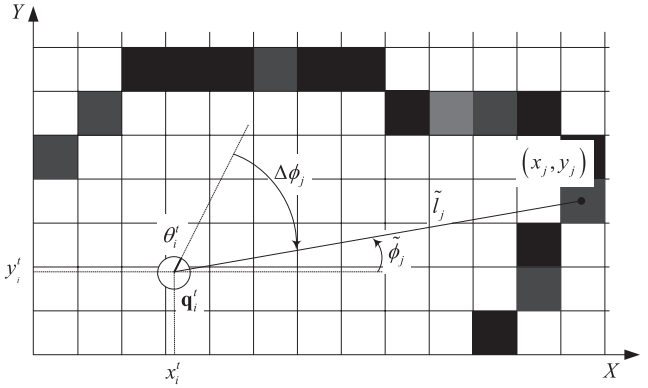

FIGURE 6 The observation model can extract the measurements $(\tilde{\mathbf{z}}_i^t)$ by the laser scanner composed of the range and bearing. For example, the j-th predicted range is determined by the distance $\tilde{l}_j$ on the bearing angle $\tilde{\phi}_j$ corresponding to the beam reflected by the closest object (x_j, y_j) in the map

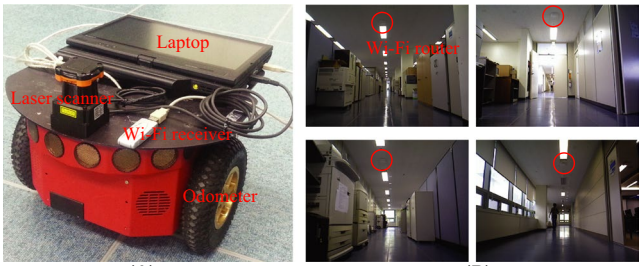

FIGURE 7 The experimental setup and the environment; (A) The mobile robot manufactured by Adept MobileRobots Co. is equipped with an odometer, a laser scanner, a Wi-Fi receiver, and a laptop computer. (B) The experimental site is an office space consisting of repeated corridors with similar spatial shapes. Wi-Fi routers are installed in the pervasive network environment to construct the smart workplace

$$\mathbf{x}^t = \left[\sum_{i=1}^{n_q^t} w_i^t x_i^t \sum_{i=1}^{n_q^t} w_i^t y_i^t \sum_{i=1}^{n_q^t} w_i^t \theta_i^t \right]. \tag{13}$$

There are various methods for solving the PF to use the weight values of the samples, for example, the best weight selection, longest survival selection, and weighted sum selection [47]. To update the robot position, the proposed method adopts the weighted sum selection using all the surviving samples.

3.3.7 | Resampling

The final step reorganizes the samples according to the new population size of the selected RSSI bins. The samples are sorted in descending order according to the weight value. The samples are divided into two parts, the parents and the offspring, with the learning rate (α) as follows:

$$\mu = (1-\alpha)\cdot n_q^t, \quad \lambda = \alpha \cdot n_q^t, \tag{14}$$

where μ and λ denote the number of parents and that of offsprings, respectively, as in the evaluation strategies [48]. The parents and the offspring groups survive and are generated, respectively. The offspring samples are randomly mutated and recombined in the pool of parent samples. All the samples are gathered for the subsequent generation as follows:

$$\mathbf{Q}_i^t \leftarrow \mathbf{Q}_i^{t,\text{parents}} \cup \mathbf{Q}_i^{t,\text{offspring}}. \tag{15}$$

4 | EXPERIMENTS AND RESULTS

A hierarchical localization framework is designed to operate regardless of the ground vehicle platform specifications such as communication protocol, driving wheel type, size, payload, and operating temperature by providing application programming interfaces (APIs) as software components. If a mobile robot is equipped with a laser scanner, a Wi-Fi receiver, and an odometer, we can apply the proposed method to accurately estimate the positions in the pervasive network environments. In particular, the proposed method is more effective for multirobot localization in a large-scale environment because each robot individually operates the localization and reduces the computational complexity.

We implemented the hierarchical localization framework to adjust the population size for reducing the amount of computation as well as for securing a robust distribution of the samples to improve the position accuracy by using the Wi-Fi network in a pervasive communication environment. We determined the input parameters of the proposed RB (RSSI bin-based) method as follows: the accuracy of RSSI bin evaluation (Σ_f) is 30 m (90 percentile accuracy of conventional fingerprint analysis) [49], error bound of RSSI bin (ε) is 5 m, number of the selected RSSI bins (s) is 6, distance interval of sample (δ) is 0.1 m, and angle interval of a sample (φ) is 15°.

In order to verify the effectiveness of the proposed method, we used a real mobile robot to perform the experiments in an office space where multiple Wi-Fi routers constitute the pervasive network environment. As shown in Figure 7A, the mobile robot is equipped with an odometer, a laser scanner, and a Wi-Fi receiver. The odometer measures the dead-reckoning position of the robot; this is used as the control input to predict the position of the samples. The laser scanner can detect the ranges and the bearing angles with respect to the surrounding objects every 0.1 second with a resolution of 0.25°, maximum range of 30 m, and coverable angle of 270°. In addition, the robot uses a Wi-Fi receiver to detect the radio signals including the MAC addresses and RSSI values. The radio signals measured by the Wi-Fi receiver are updated every 0.2 second and are utilized to evaluate the RSSI bins as the current observation. Finally, a laptop computer with a 2.8 GHz i7 processor is incorporated to store the measurement data from the sensors and to perform localization for the robot by using the proposed method.

We compared and analyzed three methods: the standard PF with a fixed sample size [18], KLD [36], and the proposed RB method. KLD and RB use the standard PF as a baseline, and each method manages the population size according to its own sampling optimization method. For an unbiased comparison, we used the same parameters for all the three methods to perform PF: the learning rate is 0.3, the standard deviation of the precision of the laser range is 0.35 m, and the accuracy of the laser range is 95%. Additionally, KLD used

the fixed parameters to reasonably adjust the sampling size according to a performance analysis as follows: the probability bound is 99%, and the error bound is 0.01 [36]. KLD can guarantee that with the specified probability bound, the KL divergence between the PF and the true distribution is less than the error bound.

As shown in Figure 7B, the experimental space is connected to numerous corridors; moreover, the object configurations are repeated with numerous similar structures. It is challenging to successfully initialize the position estimation owing to the occurrence of the local minimum in a similarly structured site. Therefore, the localization methods based on the conventional PF frequently exhibit the local minimum, although they can use a sufficient population size for the initialization. The experiment was focused on establishing the novelty of the proposed method by demonstrating whether the hierarchical localization framework can overcome the limitations of the traditional PF algorithm such as the local minimum and the large amount of computation while using the pervasive network system.

4.1 | Effects of population size

Figure 8A,B shows the procedure for analyzing the effects of the population size on the computational complexity and the success rate of the initialization of the PF. The experimental space has a physical size of 72 m × 56 m. The gray-colored region represents a space occupied by certain objects. The robot started from the bottom left and arrived at a location at the top left of the map. The robot requires the largest number of samples when it has to determine the initial position. Because the robot cannot use prior information regarding its position at the starting time, it should search the entire area and straightforwardly fall into the local minimum. Figure 8A shows an example where the robot fails to perform initialization of its position because of falling into the local minimum. Note that the experimental site consists of similar structures such as corridors and walls. The robot requires scattering of more samples in the assigned experimental space to solve the problem of the local minimum. Figure 8B indicates the initialization where the robot can estimate its position when it has moved 3 m from the starting location. This assessment condition reflects the fact that the global localization should determine the initial position of the mobile robot as rapidly as feasible to ensure navigational stability.

The initialization of the PF is repeated by 300 tests per population size of the samples. As shown in Figure 9, the probability of the initialization success is proportional to the number of samples. However, a larger population size produces a secondary effect with respect to the amount of computation. The experimental results established that the amount of computation increases with an increase in the population size of the samples. This result implies that it is necessary for the PF to adaptively regulate the population size according to the situations; for example, the population size should be increased for the initialization process and gradually decreased after completion of the initialization.

As adaptive population methods, KLD and RB can adjust the population size to perform the localization within the maximum population size that is generally assigned in the initialization process. As shown in Figure 10A, KLD regulates the number of particles according to the initially assigned population size by evaluating the quality of the particle distribution. For example, KLD allocates 50 000 particles to determine the initial position; however, it performs localization by reducing the population size to approximately 20 685 particles. Figure 10B shows the success rate and the amount of computation for KLD according to the number of initially allocated particles. Compared with the standard PF, KLD can reduce the amount of computation; however, its success rate of determining the true position is marginally lower at the population size assigned in the initialization. This is because the KLD incorrectly estimates the true distribution in the process of adjusting the population size and straightforwardly falls into the particle impoverishment at the initialization owing to an improper reduction in the population size.

Because the RB method distributes the initial particles in the candidate regions where the robot is located by using the RSSI bin evaluation, it can optimize the number of particles more effectively than the KLD can. As shown in Figure 10A, the RB reliably estimates the number of particles compared with the KLD, regardless of the initial allocated population size. This results in a high initialization success rate with a small amount of computation, as shown in Figure 10B.

4.2 | Performance of adaptive population size

We analyzed the effectiveness of the adaptive population size in improving the diversity of the distribution and reducing the computational complexity. Figure 8C shows an overview to verify the performance of the adaptive population approach. The robot moved 96 m to arrive at the destination after the initialization; the trajectories for the three methods are drawn on the map. The three trajectories appear as an overlaid one (green line); here, each method can estimate the positions of the robot from the starting to the arriving locations. The results indicate that the adaptive population methods (KLD and RB) could estimate the

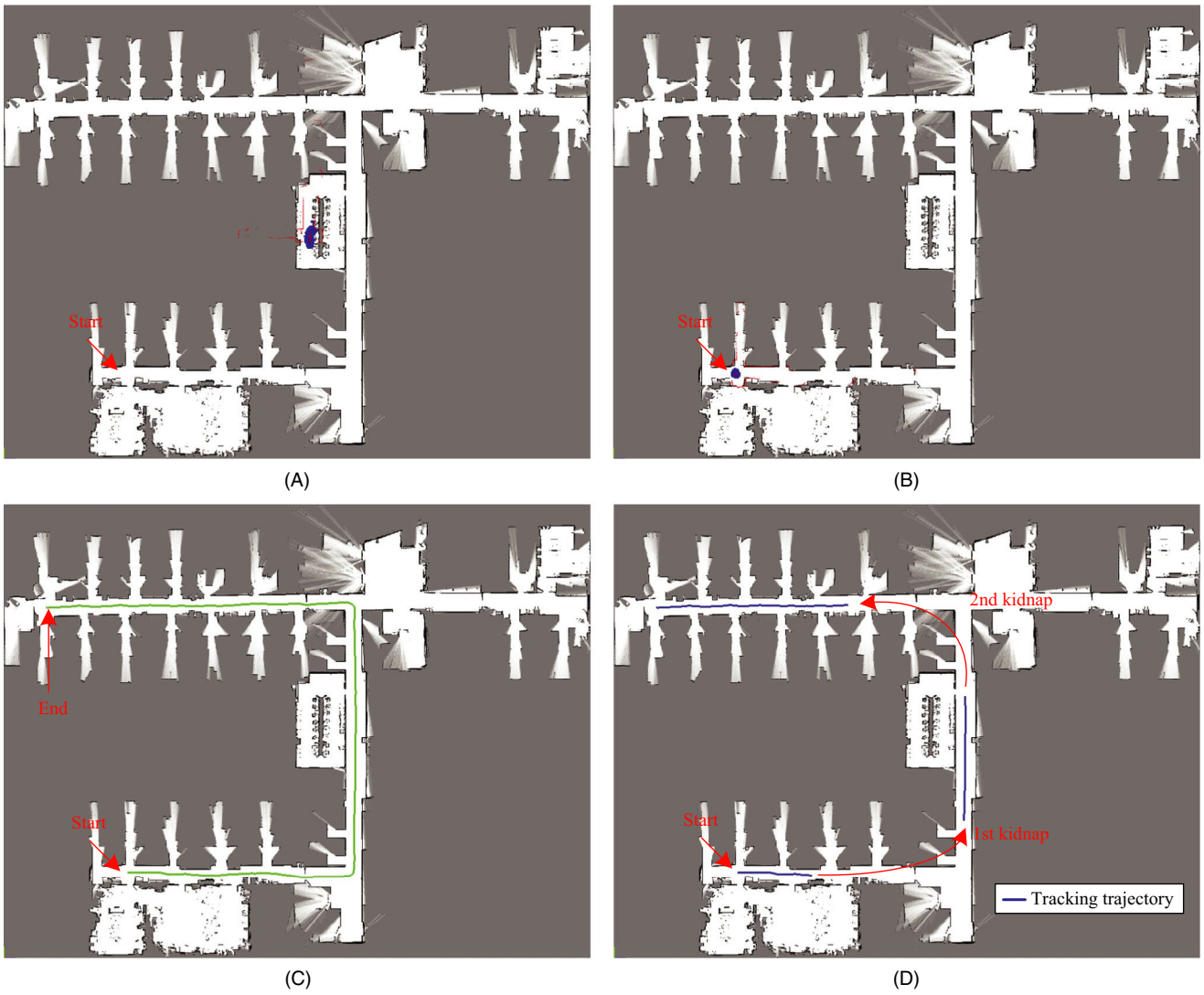

FIGURE 8 Experimental configurations; (A) When the robot moves 3 m from the starting location, it fails to determine the initial location owing to falling into the local minimum. (B) The robot can estimate the correct position for the initialization after it moves 3 m from the starting location. (C) The trajectories of the three localization methods to estimate the robot positions: the standard with fixed sample size, KLD, and the proposed RB method. The three trajectories appear as a single overlaid one (green line). This implies that the adaptive population method archives the similar performance with the fixed population method to track the positions using fewer samples after the initialization. (D) Reconstructing the starting and kidnapping situations in order to verify the performance of the global localization

correct trajectory although they used fewer samples than the standard fixed population. It is feasible for the adaptive population methods to achieve tracking performance corresponding to that of the fixed population method by using fewer samples.

We also determined that the RB method can maintain a higher diversity of the distribution than the standard and the KLD methods can for the PF. Figure 11 shows the diversity variation while the robot runs 961 iterations to estimate the positions. The three plots (of the standard, KLD, and RB methods) reveal similar progress in terms of diversity. For the average diversity value, the RB method yields 0.2140 m^2; this is marginally larger than those for the standard and KLD methods (0.2065 m^2 and 0.2063 m^2, respectively). In addition, the standard deviations of diversity are 0.0218 m^2, 0.0206 m^2, and 0.0203 m^2 for the RB, standard, and KLD methods, respectively. These results demonstrate that the RB method can maintain a more robust distribution of the samples than the other two methods.

As shown in Figure 12, the adaptive population methods optimize the sampling size according to the iteration runs. The fixed sample size of the standard PF continuously uses 50 000 samples to estimate the positions of the robot even after determining the initial location. However, KLD and RB as adaptive population methods can reduce the sample size by considering the tracking conditions

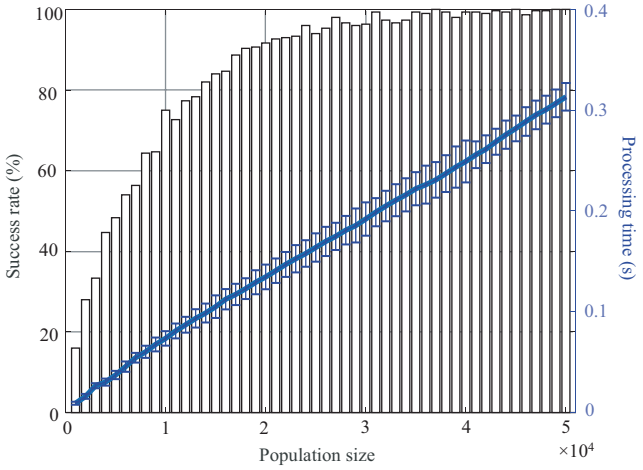

FIGURE 9 Experimental results for success rate of initialization and amount of computation for processing the standard PF, according to different population sizes

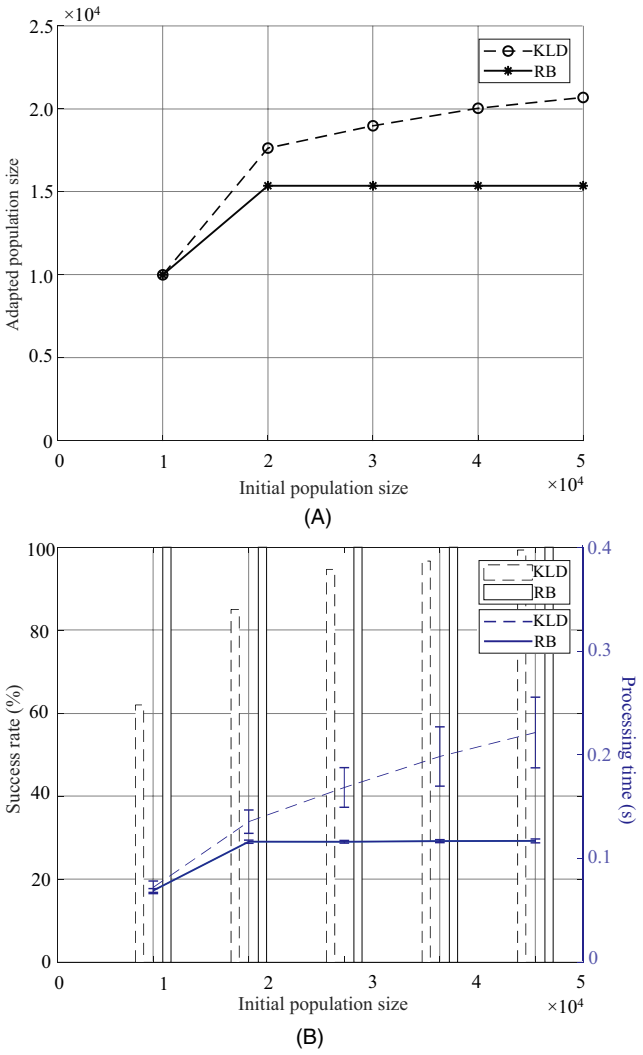

FIGURE 10 Experimental results to process KLD and RB methods according to different initial population sizes; (A) adapted population size; (B) success rate of initialization and amount of computation

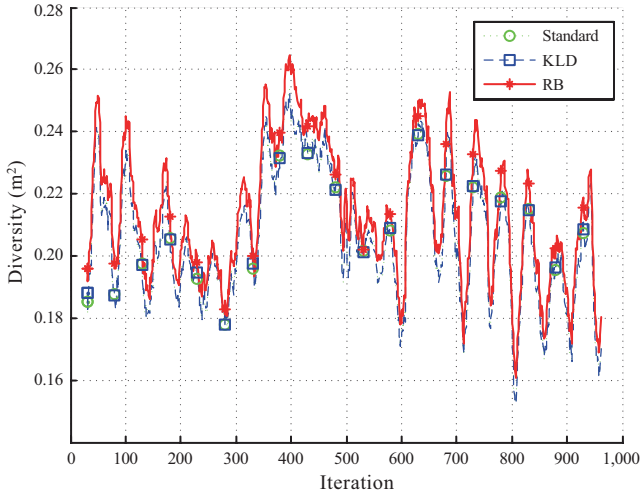

FIGURE 11 Diversity of particles for the three methods

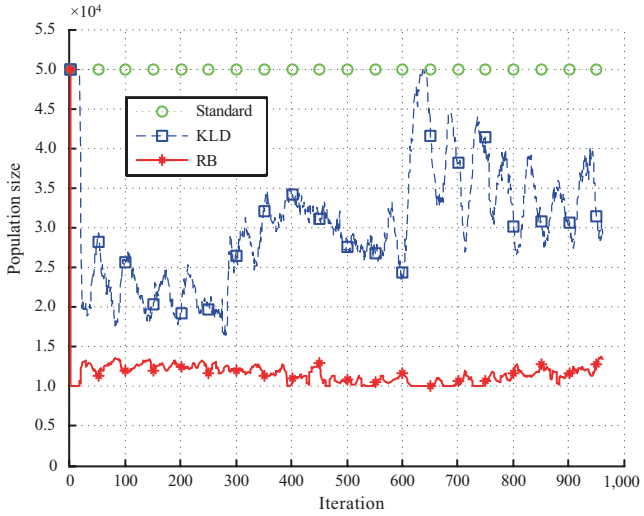

FIGURE 12 The plot shows the variation in the population size according to the iteration

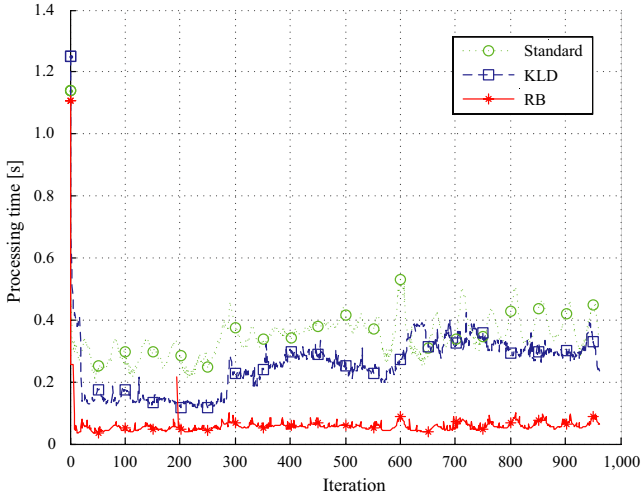

FIGURE 13 The plot shows the processing time to represent the amount of computation according to the iteration

TABLE 1 Comparison of optimization of population size

	Population size	Diversity (m^2)		Processing time (s)
	Avg.	Avg.	Stdev.	Avg.
Standard	50 000	0.2065	0.0206	0.3461
KLD	30 168	0.2063	0.0203	0.2477
RB	**11 581**	**0.2140**	**0.0218**	**0.0878**

The bold values indicate the best performance for each experiment.

after the initialization. The average sampling size of all the iterations for the standard, KLD, and RB methods are 50 000, 30 168, and 11 581, respectively, until the robot arrives at the destination. Comparing the KLD and RB methods, the KLD sensitively responds to the turning motions of the robot such as near the 290th and 600th iterations; this is because it uses the number of sample sets (the group of samples) to approximate the optimal population size. As the robot rotates, the orientation uncertainty affects the increase in the number of sample sets; furthermore, the desired sample size increases to cover the new sample sets to approximate the chi-square distribution. In the RB method, the selected RSSI bins can uniformly represent the uncertainty of the distribution regardless of the robot motions; for example, six selected RSSI bins and 5 m error boundary imply a total uncertainty of 30 m. Moreover, it is feasible to adjust the sampling size more stably in the tracking process. As a result, unlike the KLD method, the RB method can estimate the robot's positions while it undergoes rotational motion, by using a stable population size.

The adaptive population method can reduce the amount of computation by optimizing the sampling size, as shown in Figure 13. The adaptive population methods (KLD and RB) can limit the population size to less than the initial sample size in all the iterations; thereby, they should reduce the amount of computation for estimating the robot positions. The results demonstrate that the average processing time for tracking the trajectory are 0.3461, 0.2477, and 0.0878 second for the standard, KLD, and RB methods, respectively. This implies that the RB method is capable of achieving real-time localization by using the laser scanner data acquired every 0.1 second; this is because the processing time for tracking the positions is less than 0.1 second in all the iterations after initialization. Although the KLD method uses fewer samples than the standard method, it occasionally entails higher computational complexity, particularly after 600th iteration. This implies that the KLD method requires a higher computational complexity for optimizing the sampling size than for processing a reduced size of samples. Meanwhile, the RB method demonstrates consistently satisfactory results; it optimizes the population size, thereby requiring a smaller amount of computation. Two processes, the RSSI bin evaluation and the population size optimization for the RB method, require a marginal amount of computational resources.

Table 1 illustrates that the RB method can reduce the population size by approximately 76.8%, improve the diversity by approximately 3.6%, and reduce the amount of computation by approximately 74.6%, compared to the standard PF method. These results support the supposition that the RB method can achieve improvements in various aspects (specifically improvement in the diversity and reduction in the amount of computation) by managing the sample distribution.

4.3 | Performance of global localization

The performance of the global localization was evaluated by examining whether or not the initial position can be accurately estimated at the start-up, or during kidnapping or tracking failure. When the PF localization method falls into the local minimum owing to sample depletion, the robot recognizes the inaccurate global position. Therefore, the localization method should prevent the local minimum in advance because the robot cannot move without determining its initial position.

In order to verify the performance of the global localization, we carried out an experiment by setting two kidnapping situations, as shown in Figure 8D. The locations where the kidnapping occurred were set as the corridor space wherein the specific structure patterns are repeated.

TABLE 2 Comparison of estimations of global initial position: population size and success rate

	Standard		KLD		RB	
	Population size	Success rate (%)	Population size	Success rate (%)	Population size	Success rate (%)
Starting	50 000	**100.00**	20 685	99.33	**15 368**	**100.00**
1st kidnapping	50 000	85.33	38 836	89.33	**18 174**	**100.00**
2nd kidnapping	50 000	49.33	41 218	43.67	**16 974**	**84.67**

The bold values indicate the best performance for each experiment.

They are places where the PF localization method frequently fails to determine the initial position accurately. The global localization is assessed to be successful when the robot estimates its position precisely before moving 3 m from the starting point and for the two kidnapping situations. Meanwhile, if the robot cannot estimate its position although it has moved more than 3 m, the global localization is regarded as a failure. Table 2 indicates the success rate of the global localization and the average number of samples, when each situation is repeated 300 times.

Standard PF and KLD cannot provide localization framework for using the radio signals of Wi-Fi routers in a pervasive network environment; therefore, the results depended only on the measurement by the laser scanner. Meanwhile, the RB method estimates the global position by using both Wi-Fi radio signals and laser ranges. This is feasible because the RB method provides a hierarchical localization framework to fuse the two measurements (radio signals and ranges) in a pervasive network environment. It is a novelty of RB that reflects the advanced trends wherein as a part of a pervasive network, Wi-Fi devices are installed in both the robot and the space, for communication and remote control.

At the starting position, all the three methods (standard, KLD, and RB) exhibited the highest success rates owing to the unique structural shape of the space consisting of the surrounding objects. In the first and second kidnapping situations, the RB method exhibited the highest performance, with success rates of 100% and 84.67%. The RB method can reduce the probability of falling into the local minimum for the PF localization; this is because it uses the selected RSSI bins to determine the coarse locations where the robot is located. In particular, in the case of the second kidnapping, the success rates of the standard and KLD methods are significantly lower than that of the RB method; this is because the former two determine the global position by searching the whole area. The spatial structural shape of the second kidnapping is similar to the conference room in the center of the map; moreover, the standard and KLD methods were caught in the local minimum, as shown in Figure 8A. In addition, the RB method used the smallest number of samples for the initialization to determine the position.

Note that the KLD method exhibited the lowest success rate among the three methods. The main reason is that the approximation of the true distribution in KLD may be inaccurate for determining the optimal sampling size; moreover, particle depletion occurs rapidly. Through this experiment, we could verify the main advantage of RB, that is, achieving a high success rate of global localization while reducing the sampling size.

5 | CONCLUSIONS AND FUTURE WORKS

This paper describes a new hierarchical localization framework that can adaptively manage the sample distribution to estimate the global position of a robot by using the PF method, in a pervasive network environment. The key aspect of the proposed method is that the radio signals of a Wi-Fi device as one of the prevalent pervasive network devices are used to determine the region of the sample distribution. By matching the radio signals, the coarse location where the robot is situated is detected; moreover, the results are used as the boundaries to spread the samples in order to accurately determine the position in the PF localization step. By using the pervasive communication system, this approach can solve the potential problems of the conventional PF localization (ie, falling into a local minimum and a large amount of computation) with an increased sample size to cover a large-scale environment.

The hierarchical localization framework consists of three stepwise components: RSSI bin evaluation, population size optimization, and position estimation. First, the RSSI bin evaluation selects the candidate area where the robot is located by matching the radio observations and the stored RSSI bin data. Second, the population size optimization adjusts the total number of samples by using the selected RSSI bins. This can aid in maintaining a suitable amount of computation and solving the issue of the local minimum so that the robot can estimate the position in large-scale spaces. Finally, position estimation is performed to accurately determine the position of the robot with the advanced diversity of the sample distribution obtained using the PF framework.

We performed experiments to evaluate the proposed localization method in an office space where multiple Wi-Fi routers were installed to construct a pervasive network environment. A real robot was equipped with an odometer, a laser scanner, and a Wi-Fi receiver, for estimating the global position of the robot in various situations including start-up, kidnapping, and tracking. The experimental results establish that the RSSI bin-based hierarchical localization can robustly manage the diversity of the sample distribution and the adaptive size of the samples using the regions of the selected RSSI bins. In addition, the proposed method offers advantages of improving the success rate of initialization and of reducing the amount of computation compared to that of the conventional PF localization, by adjusting the distribution area and the population size of the samples. We verified that the proposed method can solve the problems of the conventional PF algorithm, such as the local minimum and the large amount of computation, as well as successfully

exploit the applicability of pervasive network devices to robot navigation.

In the future, we intend to apply the proposed method to mobile robots operating in multi-floor environments. In a multistory building space where similar structures are repeated even between different floors, the PF should use more samples than that used in a single floor, to prevent the local minimum. The proposed method can identify the region as well as the floor information where the robot exists by using the radio signals. Therefore, we look forward to the significant effect of optimizing the sampling size and improving the success rate of the global localization in multifloor environments.

ORCID

Yu-Cheol Lee https://orcid.org/0000-0003-0771-8288
Hyun Myung https://orcid.org/0000-0002-5799-2026

REFERENCES

1. P. Nazemzadeh et al., *Indoor localization of mobile robots through QR code detection and dead reckoning data fusion*, IEEE/ASME Trans. Mechatronics **22** (2017), 2588–2599.
2. M. Čáp et al., *Prioritized planning algorithms for trajectory coordination of multiple mobile robots*, IEEE Trans. Autom. Sci. Eng. **12** (2015), 835–849.
3. I. Nielsen et al., *A methodology for implementation of mobile robot in adaptive manufacturing environments*, J. Intell. Manuf. **28** (2017), 1171–1188.
4. R. Triebel et al., *Spencer: A socially aware service robot for passenger guidance and help in busy airports*, in Proc, Int. Conf. Field Service Robotics, 2016, pp. 607–622.
5. S. Azenkot, C. Feng, and M. Cakmak, *Enabling building service robots to guide blind people a participatory design approach*, in Proc. ACM/IEEE Int. Conf. Human-Robot Interaction, Christchurch, New Zealand, 2016, pp. 3–10.
6. A. Pennisi et al., *Multi-robot surveillance through a distributed sensor network*, in Proc. Cooperative Robots and Sensor Networks, 2015, pp. 77–98.
7. F. Donadio et al., *Artificial intelligence and collaborative robot to improve airport operations*, in Proc. Int. Conf. Online Eng. Internet Things, New York, USA, Mar. 2018, pp. 973–986.
8. G. Lozenguez et al., *Punctual versus continuous auction coordination for multi-robot and multi-task topological navigation*, Auton. Rob. **40** (2016), 599–613.
9. K. Hausman et al., *Cooperative multi-robot control for target tracking with onboard sensing*, Int. J. Rob. Res. **34** (2015), 1660–1677.
10. H. Yu et al., *Human—robot interaction control of rehabilitation robots with series elastic actuators*, IEEE Trans. Robot. **31** (2015), 1089–1100.
11. B. Kehoe et al., *A survey of research on cloud robotics and automation*, IEEE Trans. Autom. Sci. Eng. **12** (2015), 398–409.
12. J. A. Stankovic, *When sensor and actuator networks cover the world*, ETRI J. **30** (2008), 627–633.
13. R. Kümmerle et al., *Autonomous robot navigation in highly populated pedestrian zones*, J. Field Robot. **32** (2015), 565–589.
14. H. Kretzschmar et al., *Socially compliant mobile robot navigation via inverse reinforcement learning*, Int. J. Rob. Res. **35** (2016), 1289–1307.
15. S. Gil et al., *Adaptive communication in multi-robot systems using directionality of signal strength*, Int. J. Rob. Res. **34** (2015), 946–968.
16. K. H. Choi, Y.-S. Jeong, and J.-M. Gil, *Design and implementation of P2P home monitoring system architecture with IP cameras for a vacuum robot in ubiquitous environments*, Int. J. Sens. N. **22** (2016), 166–176.
17. P. Simoens, M. Dragone, and A. Saffiotti, *The internet of robotic things: A review of concept, added value and applications*, Int. J. Adv. Robot. Syst. **15** (2018), no. 1, 1–11.
18. S. Thrun, W. Burgard, and D. Fox, *In Probabilistic Robotics*, MIT press, 2005.
19. Z. Jiang et al., *A new kind of accurate calibration method for robotic kinematic parameters based on the extended Kalman and particle filter algorithm*, IEEE Trans. on Ind. Electron. **65** (2018), 3337–3345.
20. H. Myung et al., *Mobile robot localization with gyroscope and constrained Kalman filter*, Int. J. Control Autom. Syst. **8** (2010), 667–676.
21. M. A. Mahmud et al, *Kalman filter based indoor mobile robot navigation*, in Proc. Int. Conf. Electr., Electron. Optimization Techn., Chennai, India, Mar. 2016, pp. 1949–1953.
22. Z. Javad, Y. Cai, and Y. Majid, *Comparing EKF and SPKF algorithms for simultaneous localization and mapping*, J. Robot. N. Artif. Life **3** (2017), 217–220.
23. N. Ayadi et al., *Simulation and experimental evaluation of the EKF simultaneous localization and mapping algorithm on the Wifibot mobile robot*, J. Artif. Intell. Soft Com. Res. **8** (2018), 91–101.
24. M. Cui et al., *An adaptive unscented Kalman filter-based controller for simultaneous obstacle avoidance and tracking of wheeled mobile robots with unknown slipping parameters*, J. Intell. Robot. Syst. **92** (2018), 489–504.
25. E. Colle and S. Galerne, *A multihypothesis set approach for mobile robot localization using heterogeneous measurements provided by the internet of things*, Robot. Aut. Syst. **96** (2017), 102–113.
26. D. Liu, J. Duan, and H. Shi, *A strong tracking square root central difference FastSLAM for unmanned intelligent vehicle with adaptive partial systematic resampling*, IEEE Trans. Intell. Transp. Syst. **17** (2016), 3110–3120.
27. S. Saeedi et al., *Multiple-robot simultaneous localization and mapping: A review*, J. Field Robot. **33** (2016), 3–46.
28. D. Fox, W. Burgard, and S. Thrun, *Markov localization for mobile robots in dynamic environments*, J. of Artif. Intell. Res. **11** (1999), 391–427.
29. J. González et al., *Mobile robot localization based on ultra-wideband ranging: A particle filter approach*, Rob. Auton. Syst. **57** (2009), 496–507.
30. A. Gil et al., *Multi-robot visual SLAM using a Rao-Blackwellized particle filter*, Rob. Auton. Syst. **58** (2010), 68–80.
31. J. M. Pak et al., *Improving reliability of particle filter-based localization in wireless sensor networks via hybrid particle/FIR filtering*, IEEE Trans. Ind. Inf. **11** (2015), 1089–1098.

32. J. Jung, S.-M. Lee, and H. Myung, *Indoor mobile robot localization and mapping based on ambient magnetic fields and aiding radio sources*, IEEE Trans. Instrum. Meas. **64** (2015), 1922–1934.
33. J. Wang, P. Wang, and Z. Chen, *A novel qualitative motion model based probabilistic indoor global localization method*, Inf. Sci. **429** (2018), 284–295.
34. H. Jo et al., *Efficient grid-based Rao-Blackwellized particle filter SLAM with inter-particle map sharing*, IEEE/ASME Trans. Mechatronics **23** (2018), 714–724.
35. S. Yin and X. Zhu, *Intelligent particle filter and its application to fault detection of nonlinear system*, IEEE Trans. Ind. Electron. **62** (2015), 3852–3861.
36. D. Fox, *Adapting the sample size in particle filters through KLD-sampling*, Int. J. Rob. Res. **22** (2003), 985–1003.
37. A. W. Li and G. S. Bastos, *A hybrid self-adaptive particle filter through KLD-sampling and SAMCL*, in Proc. Int. Conf. Adv. Robot., Hong Kong, China, July 2017, pp. 1949–1953.
38. R. P. Guan, B. Ristic, and L. Wang, *Combining KLD-sampling with gmapping proposal for grid-based Monte Carlo localization of a moving robot*, in Proc Int. Conf. Inf. Fusion, Xian, China, July 2017, pp. 1–8.
39. Y. Zhang et al., *Particle swarm optimization–based minimum residual algorithm for mobile robot localization in indoor environment*, Int. J. Adv. Rob. Syst. **14** (2017), no. 5, 1–9.
40. C.-H. Chien et al, *Global localization of Monte Carlo localization based on multi-objective particle swarm optimization*, in Proc. IEEE Int. Conf. Consumer Electron., Berlin, Germany, Sept. 2016, pp. 96–97.
41. G. Tong, Z. Fang, and X. Xu, *A particle swarm optimized particle filter for nonlinear system state estimation*, in Proc, Int. Conf. Evolutionary Comput., Vancouver, Canada, July 2006, pp. 438–442.
42. Y. Li et al., *Competitive and cooperative particle swarm optimization with information sharing mechanism for global optimization problems*, Inf. Sci. **293** (2015), 370–382.
43. T. Van Erven and P. Harremos, *Rényi divergence and Kullback-Leibler divergence*, IEEE Trans. Inf. Theory **60** (2014), 3797–3820.
44. T. Li, M. Bolic, and P. M. Djuric, *Resampling methods for particle filtering: Classification, implementation, and strategies*, IEEE Signal Process. Maga. **32** (2015), 70–86.
45. Y. Suh and H. Kim, *Feature compensation combining SNR-dependent feature reconstruction and class histogram equalization*, ETRI J. **30** (2008), 753–755.
46. Y.-C. Lee, B. Park, and S. Park, *Coarse-to-fine robot localization method using radio fingerprint and particle filter*, in Proc. IEEE Int. Conf. Autom. Sci. Eng., Taipei, Taiwan, Aug. 2014, pp. 290–296.
47. T. Bäck, D. B. Fogel, and Z. Michalewicz, *In Evolutionary 1: Basic Algorithms and Operators*, Vol 1, CRC Press, Bristol, 2000.
48. N. Hansen and A. Ostermeier, *Completely derandomized self-adaptation in evolution strategies*, Evol. Comput. **9** (2001), 159–195.
49. Y. Shu et al., *Gradient-based fingerprinting for indoor localization and tracking*, IEEE Trans. Ind. Electron. **63** (2016), 2424–2433.

AUTHOR BIOGRAPHIES

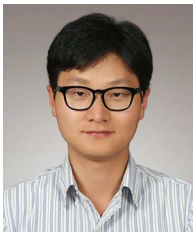

Yu-Cheol Lee received the BS degrees from both School of Mechanical Engineering and School of Electrical and Electronic Engineering of Yonsei University, Seoul, Rep. of Korea, in 2004. He received the MS degree from the Department of Mechanical Engineering of Pohang University of Science and Technology, Pohang, Rep. of Korea, in 2006. Since 2006, he has been a senior researcher with Intelligence and Robot System Research Group in Electronics and Telecommunications Research Institute, Daejeon, Rep. of Korea. He is presently pursuing the PhD degree in Robotics Program from the Korea Advanced Institute of Science and Technology, Daejeon, Republic of Korea. He has participated in numerous large-scale research projects in a leadership role as a researcher and manager. His research achievements have been presented at/in prominent international conferences and journals including IEEE, ASME, RSJ, and KRoS, wherein he has received outstanding research awards. Presently, his research interests include localization and map building for intelligent vehicles, and navigation technology for pedestrians in indoor and outdoor environments.

Hyun Myung received the BS, MS, and PhD degrees in electrical engineering from the Korea Advanced Institute of Science and Technology (KAIST), Daejeon, Rep. of Korea, in 1992, 1994, and 1998, respectively. He was a senior researcher with the Electronics and Telecommunications Research Institute, Daejeon, Rep. of Korea from 1998 to 2002; a chief technology officer and the director with the Digital Contents Research Laboratory, Emersys Corporation, Daejeon, Rep. fo Korea, from 2002 to 2003; and a principle researcher with the Samsung Advanced Institute of Technology, Yongin, Rep. of Korea, from 2003 to 2008. Since 2008, he has been a professor with the Department of Civil and Environmental Engineering, KAIST. He is also the head of the KAIST Robotics Program. From 2019, he is a professor with the School of Electrical Engineering. His current research interests include simultaneous localization and mapping, robot navigation, machine learning, artificial intelligence, deep learning, swarm robot, and structural health monitoring using robotics.